Nonlinear Dynamics and Systems Theory, **24** (1) (2024) 12–27

A General Kinematic-Based Walking Algorithm of a Hexapod Robot on Irregular Terrain

A. Aissaoui [1*], C. Mahfoudi [2] and S. Djeffal [2]

[1] *University of Oum El bouaghi, Algeria.*
[2] *University of Oum El bouaghi, CMASMTF laboratory, Algeria.*

Received: March 7, 2023; Revised: December 31, 2023

Abstract: Developing an algorithm for ensuring a feasible gait of Hexapod Walking Robots (HWRs) poses the challenge of enabling smooth locomotion on uneven terrain, utilizing the mobility of its six legs that alternately make contact with the ground. To this end, a kinematic-based approach is applied that individually takes into account the movements of each leg, while maintaining compatibility with the body's motion through a non-symmetrical tripod gait. Accordingly, the forward kinematics of the robot is established using the Denavit-Hartenberg parameterization and its inverse kinematics is derived using Paul's method. Then, the uneven terrain is represented by elevation differences in a 3D curve trajectory. After that, an algorithm is proposed to ensure the adaptability of the robot's legs with respect to the terrain's shape, namely, the algorithm allows each leg to follow its own trajectory independently. To validate the proposed approach, 3D simulations are conducted using MATLAB software, demonstrating the accuracy and reliability of the purely kinematic approach. The results show that the algorithm enables the HWR to adapt its walking to irregular terrain in various general cases.

Keywords: *Hexapod Walking Robots (HWRs); modeling robots; gait locomotion; tripod gait.*

Mathematics Subject Classification (2010): 70K25, 70K42, 70K70, 93-04, 93-10.

* Corresponding author: mailto:aissaoui.abderahmane@univ-oeb.dz

1 Introduction

Hexapod Walking Robots (HWRs) are mechanical vehicles that emulate the locomotion of insects, characterized by their mobility, maneuverability, adaptability, flexibility, and stability in natural terrains. These robots are inspired by the biological features of insects and utilize six legs for walking, enabling them to navigate various terrains with efficiency and versatility [1,2]. In legged locomotion, HWRs are favored by static stability gait due to having three legs in contact with the ground all the time, flexibility where they move, fault tolerant locomotion, possibility to manipulate objects using their legs as arms.

In addition to the advantages mentioned earlier, Hexapod Walking Robots (HWRs) have superior terrain adaptation capabilities compared to wheeled robots. By utilizing discrete contacts with the ground, HWRs can bypass undesirable footholds, avoid obstacles, select optimal terrain contacts, and adapt their walking posture to navigate through confined spaces. This is made possible due to their high degrees of freedom and flexibility, which make them the ideal solution for locomotion on rough and uneven terrains. HWRs have a unique advantage in navigating complex environments and are well-suited for applications that require versatile and agile mobility in challenging terrains [3–5]. HWRs can be used for intervention in hostile environments like humanitarian demining operations, disaster recovery missions, nuclear plant maintenance, operations in volcanic sites, underwater searching and space exploration. Beyond this type of applications, HWRs can also be used in a wide variety of service tasks such as forest harvesting and service robots [6–9].

In current realizations, hexapod robots are very far from the complexity of real insects in terms of the number of degrees of freedom, velocity and dimensions. Researchers are only interested in extracting the essential characteristics of the insects' walking system and implementing them in real robots. A gait can be described as a sequence of leg motions coordinated with a sequence of body motions for transporting the robot's body [10]. The choice of the gait's mode is the first essential step to guarantee stability and efficiency of the hexapod walking robot motion.

Most studies used for hexapod locomotion the common and basic gait called a tripod gait where the body is propelled continuously by the cyclic sequencing of the movements of three legs which were in the air and come to rest on the ground while the other three release the contact there and return after half a period (legs coordination). Each leg performs a walking step in two phases [11]: a support phase during which the foot of the leg remains in contact with the ground, its active joints cause the robot's body to move forward horizontally; and a swing phase where the end of the leg follows a trajectory in the air and then comes back into contact with the ground to start a new step. This tripod gait of the hexapod can achieve fast movement with stability.

In terms of the hexapod robot's gait generation, we note that the legged locomotion of the HWRs is performed according to two major types of approaches: analytical approaches and bio-inspired approaches. Since it does not require complex geometrical calculation, the majority of studies are made according to the bio-inspired approaches to generate symmetrical gaits and reproduce different type of gaits for a hexapod robot. The most common approach for the design of a bio-inspired architecture consists of a Central Pattern Generator (CPG) network with six coupled nonlinear oscillators [12]. By controlling the durations of the ascending and descending phase of the limb trajectory, they control the durations of the swing and stance step phases, respectively. This network produces synchronized rhythms that give the correct pattern for locomotion [13, 14].

As regards the analytical approaches, we note firstly that the existing works regarding gait generation in flat terrain, only deal with a single X direction and describe the kinematic model by using a matrix approach and propose different gaits (tripod gait, quadrangular gait, and pentagonal gait) where the sequences of coordination legs according to different rhythms are converted by the Inverse Kinematics Model (IKM) and preloaded on a computer which sends commands to the servo controller and the hexapod executes corresponding instructions [10, 15–17]. The models mentioned above only work on flat ground and constitute a compulsory phase to begin with, but in reality, it is necessary to take into account, during the modeling, the nature of the real terrain which is uneven and which presents irregularities.

A synthesis of the works quoted above allowed us to notice that the generation of trajectories of HWRs on an uneven ground which presents irregularities in terms of variation of altitude is an extension of walking on flat ground, which is a reduced case of walking. For this, we are motivated by the study of the general case of real walking which can model at the same time and in an exact mathematical way the HWRs with all its 24 degrees of freedom in walking interaction on a rough terrain of arbitrary shape which can be modeled by a 3D curve without any restriction either on the model of the robot or on the terrain. The rest of the paper is structured as follows. Section 2 presents the kinematic modeling of the HWR. The proposed walking algorithm is studied in detail in Section 3. Section 4 illustrates the results obtained using this approach. Finally, conclusions are made in Section 5.

2 HWR Model

A hexapod walking robot consists of a rectangular body to which six identical legs are articulately attached, see Figure 1. Each leg of the robot has three degrees of freedom allowing the robot to move its legs dexterously according to the given position within its workspace.

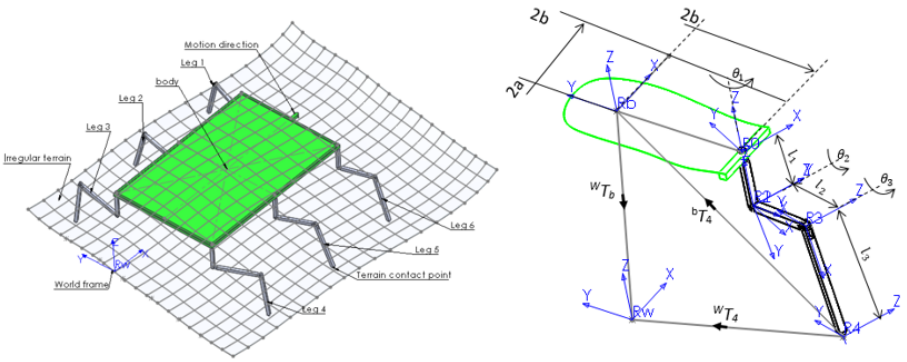

Figure 1: (Left) CAD Model of the HWRs with six legs; (Right) Attachment of the reference frames for the robot's five legs as a model.

2.1 Forward kinematic model of the hexapad robot

The forward kinematic model (FKM) [18–20] for a hexapod robot resides in finding the location of robot body with respect to robot's legs joint variables according to the

coordinate frames established in Figure 1 (right). To model the HWRs having a body of length $2a$ and a width $2b$, the leg number five is chosen as the leg-model [21]. It is made up of three segments of respective lengths l_1, l_2, l_3 and three rotoid articulations of angle θ_1, θ_2 and θ_3. The D-H parameters of the leg-model are shown in equation (6). The FKM of a leg relative to the world frame is calculated by the product of the homogeneous transformation matrices according to equation (1), namely it provides the positions of the contact points of each leg according to the world frame.

$$ {}^{W}T_{4,j} = {}^{W}T_{b}\,{}^{b}T_{0,j}\,{}^{0,j}T_{1,j}\,{}^{1,j}T_{2,j}\,{}^{2,j}T_{3,j}\,{}^{3,j}T_{4,j} \tag{1} $$

with $j = \overline{1,6}$ being the legs' index.

The matrix situation of the robot's base can be expressed as follows:

$$ {}^{W}T_{b} = {}^{W}Trans_{b}\,{}^{W}Rot_{b}(Z_{\psi}, Y_{\theta}, X_{\varphi}) \tag{2} $$

with

$$ {}^{0}Trans_{b} = \begin{bmatrix} 1 & 0 & 0 & x_b \\ 0 & 1 & 0 & y_b \\ 0 & 0 & 1 & z_b \\ 0 & 0 & 0 & 1 \end{bmatrix}. \tag{3} $$

The matrix of articulations points of each leg can be expressed by the following:

$$ {}^{b}T_{0,j} = \begin{bmatrix} 1 & 0 & 0 & x_{0,j} \\ 0 & 1 & 0 & y_{0,j} \\ 0 & 0 & 1 & z_{0,j} \\ 0 & 0 & 0 & 1 \end{bmatrix}, \tag{4} $$

$$ \begin{aligned} x_{0,j} &= \begin{bmatrix} -a & -a & -a & a & a & a \end{bmatrix}, \\ y_{0,j} &= \begin{bmatrix} b & b & b & -b & -b & -b \end{bmatrix}, \\ z_{0,j} &= \begin{bmatrix} 0 & 0 & 0 & 0 & 0 & 0 \end{bmatrix}. \end{aligned} \tag{5} $$

The parameters table of Denavit-Hertberg corresponding to the leg_j is

$$ DH_j = \begin{bmatrix} 0 & 0 & \theta_{1,j} & -l_1 \\ -\pi/2 & 0 & \theta_{2,j} & 0 \\ 0 & l_{2,j} & \theta_{3,j} & 0 \\ 0 & l_{3,j} & 0 & 0 \end{bmatrix}. \tag{6} $$

The homogenous matrix of Denavit-Hertberg can be expressed as follows:

$$ {}^{j-1}T_{j} = \begin{bmatrix} C\theta_j & -S\theta_j & 0 & d_j \\ C\alpha_j S\theta_j & C\alpha_j C\theta_j & -S\alpha_j & -r_j S\alpha_j \\ S\alpha_j S\theta_j & S\alpha_j C\theta_j & C\alpha_j & r_j C\alpha_j \\ 0 & 0 & 0 & 1 \end{bmatrix} \tag{7} $$

$$ with\ C(.) = Cos(.)\ ,\ S(.) = Sin(.). $$

Four matrices of the leg-model are worth, respectively,

$$ {}^{0}T_{1} = \begin{bmatrix} C1 & -S1 & 0 & 0 \\ S1 & C1 & 0 & 0 \\ 0 & 0 & 1 & -l1 \\ 0 & 0 & 0 & 1 \end{bmatrix}, \tag{8} $$

$$ {}^{1}T_2 = \begin{bmatrix} C2 & -S2 & 0 & 0 \\ 0 & 0 & 1 & 0 \\ -S2 & -C2 & 0 & 0 \\ 0 & 0 & 0 & 1 \end{bmatrix}, \tag{9} $$

$$ {}^{2}T_3 = \begin{bmatrix} C3 & -S3 & 0 & l2 \\ S3 & C3 & 0 & 0 \\ 0 & 0 & 1 & 0 \\ 0 & 0 & 0 & 1 \end{bmatrix}, \tag{10} $$

$$ {}^{3}T_4 = \begin{bmatrix} 1 & 0 & 0 & l3 \\ 0 & 1 & 0 & 0 \\ 0 & 0 & 1 & 0 \\ 0 & 0 & 0 & 1 \end{bmatrix}. \tag{11} $$

This yields the FKM of leg model 5 (Figure 2).

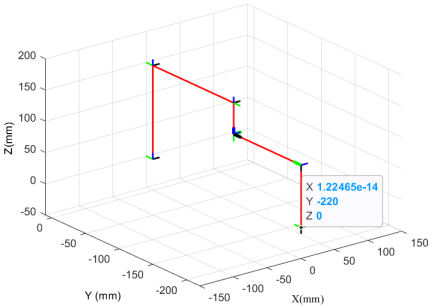

Figure 2: FKM of the leg model 5.

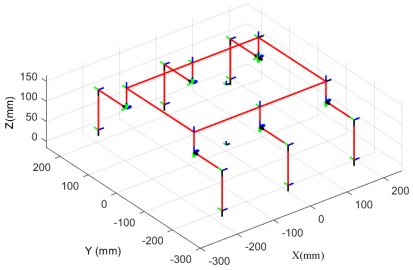

Figure 3: HWR's FKM.

After calculating the FKM of the leg-model, the FKM of the entire robot consists in distributing six legs around its body as it is shown in Figure 3.

2.2 Inverse kinematic model of hexapod robot

The inverse kinematic model (IKM) of the HWR's leg is firstly calculated according to the body frame R_b. As previously mentioned, the FKM of the robot can be expressed by the following equation:

$$ U_0 = \begin{bmatrix} s_x & n_x & a_x & PX \\ s_y & n_y & a_y & PY \\ s_z & n_z & a_z & PZ \\ 0 & 0 & 0 & 1 \end{bmatrix} = {}^{b}T_{0,j}\,{}^{0,j}T_{1,j}\,{}^{1,j}T_{2,j}\,{}^{2,j}T_{3,j}\,{}^{3,j}T_{4,j}. \tag{12} $$

Paul's method consists in multiplying the equation (12) by ${}^{1,j}T_b$ which is the inverse of ${}^{b}T_{1,j}$:

$$ {}^{1,j}T_b U_0 = {}^{1,j}T_{2,j}\,{}^{2,j}T_{3,j}\,{}^{3,j}T_{4,j}, \qquad j = \overline{1,6}. \tag{13} $$

By identifying the elements of the fourth column of the product on the left-hand side of equation (13) with those of the fourth column of the product on the right, we will have

$$ S1 = PY - y_{0,j},\ S1 = PX - x_{0,j}, $$
$$ \theta_1 = ATAN2(S1, C1),\ \theta_1^{'} = \theta_1 + \pi. $$

The second multiplication yields

$$
\begin{aligned}
&X = (PX - x_{0,j})C1 + (PY - y_{0,j})S1 \ , \\
&Y = PZ + l_1 \, , \ \ Z_1 = -l_2 \ , \ Z2 = 0 \ , \ \ W = l_3, \\
&B1 = -2(XZ2 + YZ1) \ , B2 = 2(XZ1 - YZ2), \\
&B3 = W^2 - X^2 - Y^2 - Z1^2 - Z2^2, \\
&S2 = (B1B3 + B2(B1^2 + B2^2 - B3^2)^{0.5})/(B1^2 + B2^2), \\
&C2 = (B2B3 - B1(B1^2 + B2^2 - B3^2)^{0.5})/(B1^2 + B2^2), \\
&\theta_2 = ATAN2\,(S2, C2)\,,
\end{aligned}
$$

$$
\begin{aligned}
S3 &= (-XS2 - YC2 + Z2)/W, \\
C3 &= (XC2 - YS2 + Z1)/W, \\
\theta_3 &= ATAN2(S3, C3)\,.
\end{aligned}
$$

The hexapod robot simulation via MATLAB is executed to verify the efficiency of the derived IKM with different curbs followed by the robot leg points of contact. As it is shown in Figures 4, 5, 6, 7, the robot's leg follows spatial straight line, circle-like shape, cycloid and spiral trajectories, respectively.

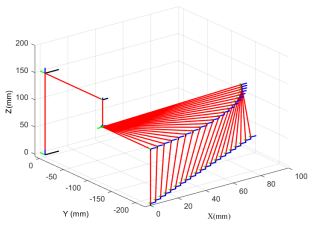

Figure 4: The robot's leg follows spatial linear trajectory.

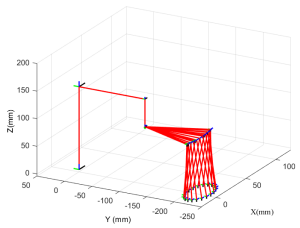

Figure 5: The robot's leg follows circular trajectory.

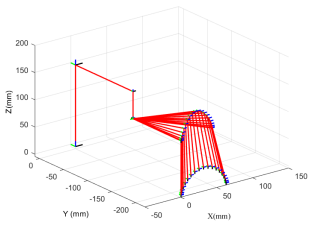

Figure 6: The robot's leg follows cycloid trajectory.

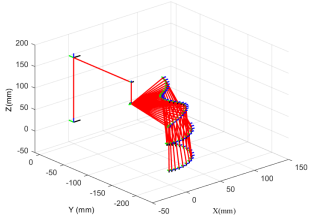

Figure 7: The robot's leg follows spiral trajectory.

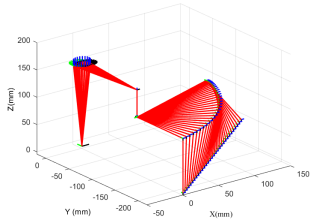

Figure 8: Simultaneous movement of the leg's point of contact (linear) and body of the robot (circular).

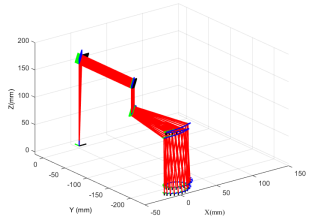

Figure 9: Simultaneous movement of the leg's point of contact (spiral) and body of the robot (linear-spatial).

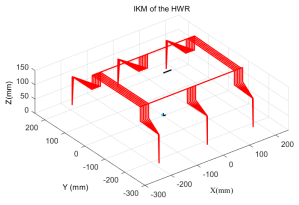

Figure 10: Linear trajectory along X.

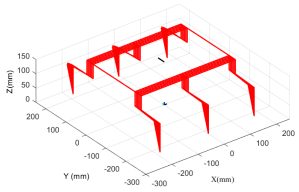

Figure 11: Linear trajectory along Y.

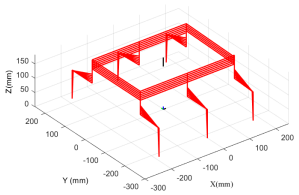

Figure 12: Linear trajectory along Z.

Additionally, the movement of robot's leg point of contact can be performed simultaneously with that of the body as is depicted in Figures 8, 9.

Finally, we validate the established IKM of the whole robot, namely the robot's body can perform six degrees of freedom $(x_b, y_b, z_b, Z_\psi, Y_\theta, X_\varphi)$, meanwhile its legs can further move according to any given trajectory belonging to the robot's workspace as it is graphically represented in Figures 10, 11, 12, 13, 14, 15.

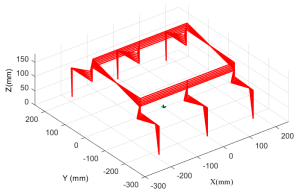

Figure 13: HWR's body rotation ϕ around X

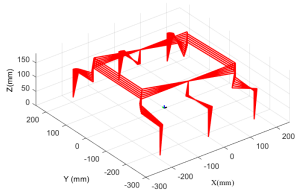

Figure 14: HWR's body rotation θ around Y

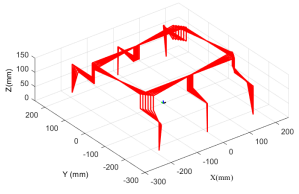

Figure 15: HWR's body rotation ψ around Z

.

In conclusion, for the HWR's IKM, an example is given in Figure 16 which represents the eighteen values of the angles $(\theta_1, \theta_2, \theta_3)$ of the HWR's six legs corresponding to the posture of Figure 16 previously presented.

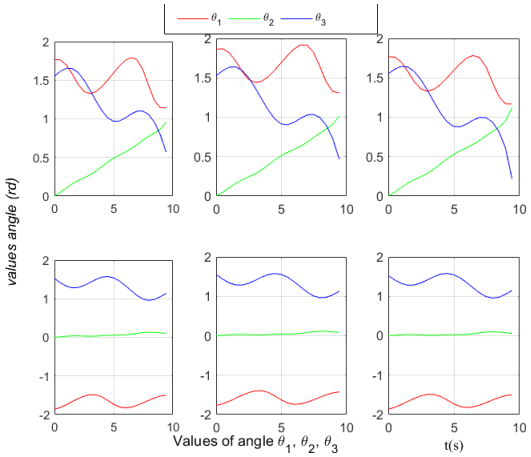

Figure 16: Values of angles $(\theta_1, \theta_2, \theta_3)$ which correspond to the posture of Figure 15.

3 Proposed Walking Algorithm of a HWR on Irregular Terrain

The generation of the walk of an HWR on irregular terrain must take into account, in addition to the modeling of the robot, the irregular shape of the terrain which is manifested by differences in altitudes of the contact points with the ground. These differences express the variation of the Z component of these contact points which is zero for a flat terrain and different from zero for irregular terrain. To achieve this objective of walking on irregular terrain, we propose in this paper a general algorithm that works according to the following flowchart.

- Step 1: input: Geometrical parameters of the HWR (a=180; b=120; l1=50; l2=100; l3=100).
- Step 2: input: Any 3D terrain composed of 6 trajectories, each comprising n_{steps}.
- Step 3: Model of irregular terrain and extraction of its parameters.
  - ✓ for each step k (k=1: n_{steps}) do:
    - ✓ for t=0:n (n refers to the step's period)
    - ∗ *if t≤n/2 do*
  - − for each leg$_j$ ($j = 1 : 6$) do:
- Step 4: Adaptation of the Normal Cycloid$_j$ (NC)$_j$ (leg$_j$: $j = 1, 3, 5$) to its irregular terrain$_j$.
- Step 5: Adaptation of leg$_j$ to follow the Adapted Cycloid$_j$ (AC)$_j$.
- Step 6: Synchronization of the movements of six legs (tripod gait: 135_{swing} and 246_{stanse}).
- Step 7: Adaptation of the movement of the HWR's body to the movements of its six legs.
- Step 8: IKM of leg$_j$.
- Step 9: FKM of leg$_j$.
- Step 10: End for each leg$_j$.
- if t>=n/2: do
- Step 11: Actualization of body position.
- for each leg$_j$ do
- Step 12: Adaptation of the Normal Cycloid$_j$ (NC)$_j$ (leg$_j$: $j = 2, 4, 6$) to its irregular terrain$_j$.
- Step 13: Adaptation of leg$_j$ to follow the Adapted Cycloid$_j$ (AC)$_j$.
- Step 14: Synchronization of the movements of six legs (tripod gait: 246_{swing} and 135_{stanse}).

- Step 15: Adaptation of the movement of the body of the HWR to the movements of its six legs.
- Step 16: IKM of leg_j.
- Step 17: FKM of leg_j.
- End for each leg$_j$.
- End for t=0:n.
- End for each step k.

It is noteworthy to say that the aforementioned algorithm's steps for HWR walking are elaborately detailed in the following sections.

3.1 Model of the irregular terrain and extraction of its parameters

In general, the walking of a hexapod walking robot (HWR) may not be symmetrical, and each leg may follow a different trajectory compared to the others. To account for this, we define the model of the irregular terrain for each leg as a set of contact points belonging to a 3D curve. As a result, the irregular terrain can be represented by six curves, within the reachable domain of the robot, derived from the shape of the reference terrain, which is defined by

$$\begin{cases} x_T, \\ y_T = f_x\left(x_T\right), \\ z_T = f_{xy}\left(x_T, y_T\right), \end{cases} \tag{14}$$

with

- x_T : Evolution of the terrain along the X axis with a step length and a number of n_{step};
- f_x : A function of x_T representing the evolution of the terrain along the Y axis;
- f_{xy} : A function of x_T and y_T denoting the variation in altitude of different points of the terrain.

The position of six legs relative to the reference is given by the matrix T_{R1} as

$$T_{R1} = \begin{bmatrix} x_T + a & y_T + (b + l2) & z_T \\ x_T - pas/2 & y_T + (b + l2) & z_T \\ x_T - a & y_T + (b + l2) & z_T \\ x_T - a - pas/2 & y_T - (b + l2) & z_T \\ x_T & y_T - (b + l2) & z_T \\ x_T + a - pas/2 & y_T - (b + l2) & z_T \end{bmatrix}^T . \tag{15}$$

Then, we distinguish between these six identical trajectories by introducing the following coefficients $k_{i,j}$:

$$T_{Rk} = \begin{bmatrix} k_{11}x_T + a & k_{21}y_T + (b + l2) & k_{31}z_T \\ k_{12}x_T + pas/2 & k_{22}y_T + (b + l2) & k_{32}z_T \\ k_{13}x_T - a & k_{23}y_T + (b + l2) & k_{33}z_T \\ k_{14}x_T - a - pas/2 & k_{24}y_T - (b + l2) & k_{34}z_T \\ k_{15}x_T & k_{25}y_T - (b + l2) & k_{35}z_T \\ k_{16}x_T + a - pas/2 & k_{26}x_T - (b + l2) & k_{36}z_T \end{bmatrix}^T . \tag{16}$$

Remarkably, T_{Rk} can describe any type of irregular terrains that the HWR can track according to the given values of the coefficients k_{ij} :

- $k_{ij} = 1$ for a reference terrain;
- $k_{3j} = 0$ for flat terrain;
- Remaining case for any uneven terrain.

Figure 17 illustrates 6 independent trajectories corresponding to six legs of the HWR:

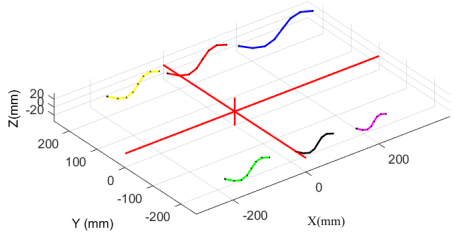

Figure 17: 6 curves representing 6 trajectories to follow.

For each terrain$_j$ composed of n_{steps} that the leg$_j$ must follow, we calculate the geometric parameters of two contact points P_O (x_{T0j}, y_{T0j}, z_{T0j}) of the beginning and P_1 (x_{T1j}, y_{T1j}, z_{T1j}) of the end of a walking step (see Figure 18) according to

$$\Psi_j = -\operatorname{atan2}\left(\left(y_{T1j} - y_{T0j}\right), \left(x_{T1j} - x_{T0j}\right)\right), \tag{17}$$

$$lp_j = \sqrt{\left(x_{T1j} - x_{T0j}\right)^2 + \left(y_{T1j} - y_{T0j}\right)^2}, \tag{18}$$

$$\Theta_j = \operatorname{atan2}\left(\left(z_{T1_j} - z_{T0_j}\right), lp_j\right), \tag{19}$$

$$ls_j = \sqrt{\left(x_{T1_j} - x_{T0j}\right)^2 + \left(y_{T1j} - y_{T0j}\right)^2 + \left(z_{T1j} - z_{T0j}\right)^2}, \tag{20}$$

$$R_j = \frac{ls_j}{2 \times \pi}, \tag{21}$$

Ψ_j : the rotation angle along OZ;
lp_j : the length of the step in the plane XOY;

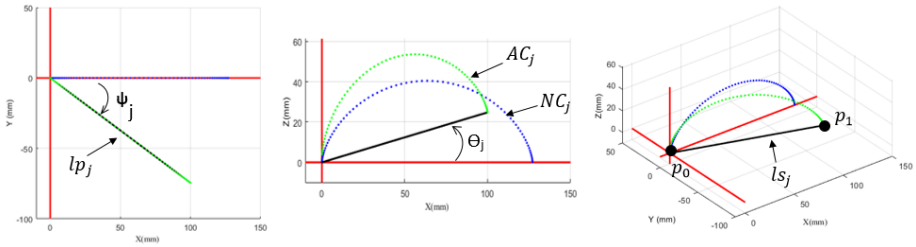

Figure 18: Adaptation of the cycloïd 5 to the irregular terrain at the origin XY.

Θ_j : the rotation angle along OY;
ls_j : the length of the step in the space;
R_j : the cycloid' radius.

3.2 Adaptation of the normal cycloid$_j$ to the irregular terrain$_j$

We define a Normal Cycloid$_j$ trajectory in the XOZ plane (Figure 19)that the leg$_j$ must follow in the swing phase by the following equation:

$$\begin{cases} x_{NCj} = R_j \times (t - \sin(t)), \\ y_{NCj} = 0, \\ z_{NCj} = R_j \times (1 - \cos(t)). \end{cases} \tag{22}$$

We adapt the normal cycloid NC_j so that it matches its terrain$_j$ by the combination of two rotations and a translation (Figure 20) and it is denoted AC_j, thus it is adapted to the terrain$_j$ by the relations

$$AC_j = NC_j \times rot(Y, \Theta_j) \times rot(Z, \Psi_j) + [x_{T0j}; y_{T0j}; z_{T0j}], \tag{23}$$

$rot(Z, \Psi_j)$: Rotation matrix around OZ;
$rot(Y, \Theta_j)$: Rotation matrix around OY.

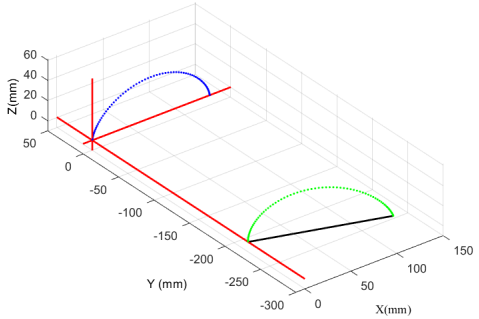

Figure 19: Adaptation of the cycloid$_5$ to the irregular terrain$_5$ for one step.

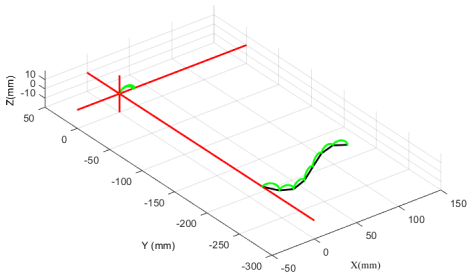

Figure 20: Adaptation of the cycloid to uneven terrain composed of seven steps.

3.3 Adaptation of leg$_j$ to the cycloid of its terrain$_j$

Depending on the desired number of steps, each leg$_j$ follows the cycloids adapted with a fixed body (see Figure 21) using the developed IKM.

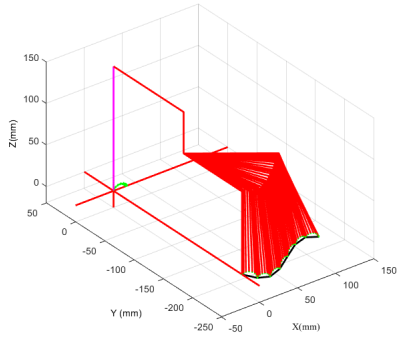

Figure 21: Adaptation of the leg$_j$ to the cycloids of its terrain$_j$.

3.4 Synchronization of the movements of six legs in the tripod mode

Each leg of the HWR performs a walking step in two phases: a support phase and a swing phase (see Figure 22). The most used mode of walking which can ensure speed and stability is the alternating tripod, it is carried out by the sequencing of six legs, three by three during a period T: in the first half-period, the legs 135 are in the swing phase and legs 246 are in the support phase as they alternate in the second half-period for one and seven walking steps, respectively. Furthermore, for instance, the synchronization is given between two consecutive legs number five and six (see Figure 23).

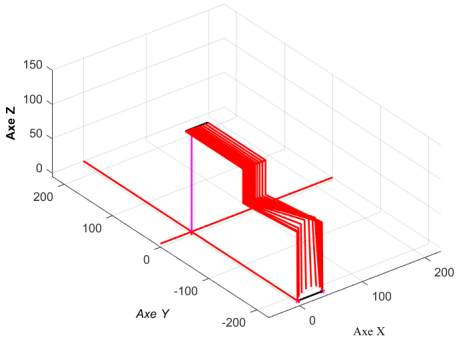

Figure 22: Two phases of a leg$_j$ for one walking step.

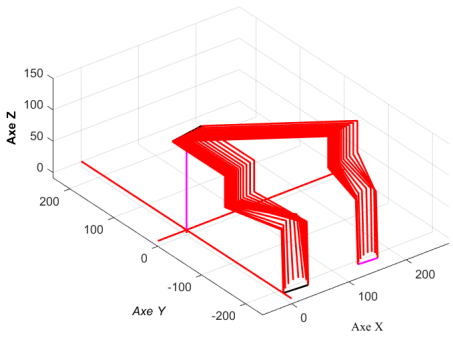

Figure 23: Synchronisation of a walking step for legs 5 and 6.

3.5 Adaptation of body's movement to the movements of its six legs

The spatial displacement of the body of the HWR occurs when the legs in contact with the ground propel it into a given coherent situation (position and orientation). To ensure

the compatibility between the movement of the legs and that of the body, we propose for the body:

- movement in the XOY plane in small straight segments as the average resultant of the movement of six legs along

  ✓ the X axis:

$$\begin{cases} x_{T0} = \sum_{j=1}^{6} \frac{x_{T0j}}{6}, \\ x_{T1} = \sum_{j=1}^{6} \frac{x_{T1j}}{6}, \\ x_b = \frac{x_{T1}-x_{T0}}{2n} t + x_{00}, \end{cases} \tag{24}$$

  where x_{00} refers to the initial position of the robot's body;

  ✓ the Y axis:

$$\begin{cases} y_{T0} = \sum_{j=1}^{6} \frac{y_{T0j}}{6}, \\ y_{T1} = \sum_{j=1}^{6} \frac{y_{T1j}}{6}, \\ y_b = \frac{y_{T1}-y_{T0}}{x_{T1}-x_{T0}} x_b + y_{T0} - \frac{(y_{T1}-y_{T0})}{(x_{T1}-x_{T0})} x_{T0}; \end{cases} \tag{25}$$

- the Z axis, a sinusoidal [22,23] movement (see Figure 25) which describes the case of the real gait of the insect and that at a fixed height (see Figure 24) of its body.

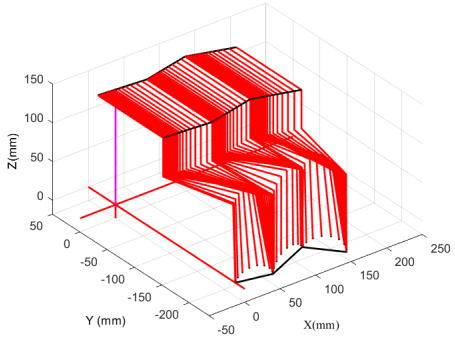

Figure 24: Alternating tripod gait of the HWR on flat terrain at a fixed height of the body.

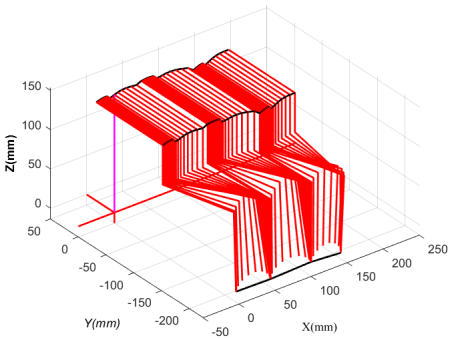

Figure 25: Alternating tripod gait of the HWR on flat terrain with sinusoidal height of the body.

4 Results and Discussion

In this section, the obtained results are mainly based on three types of terrain progressively ordered by the degree of locomotion's difficulty:

- A flat terrain is characterized by its null altitude ($Z = 0$). It is obviously clear from (Figure 26), the HWR executes two steps of alternating tripod walking while its body remains horizontal at a constant height $(l1+l3)$ and it oscillates horizontally (see Figure 27).

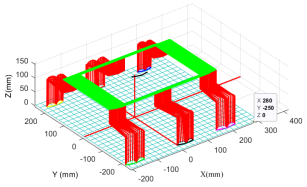

Figure 26: Alternating tripod gait of the HWR on flat terrain at a fixed height of the body.

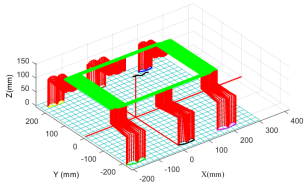

Figure 27: Alternating tripod gait of the HWR on flat terrain with a sinusoidal height of the body.

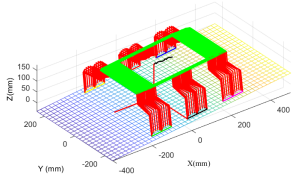

Figure 28: Alternating tripod gait of the HWR on inclined terrain with sinusoidal movement while the body remains parallel to the sloped terrain.

- On slopped terrain, in this simulation, the HWR executes two steps of alternating tripod gait on an inclined plan and it oscillates sinusoidally and remains parallel to terrain (see Figure 28).
- An irregular terrain with a constant and variable height of the body (see Figures 29 and 30).

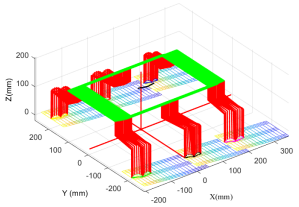

Figure 29: Walking on uneven ground at a fixed body height.

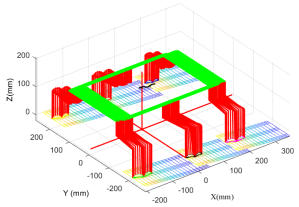

Figure 30: Walking on irregular terrain with sinusoidal height of the body.

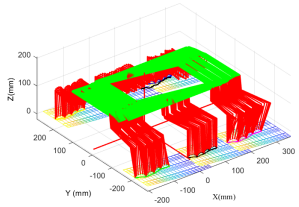

Figure 31: Walking on irregular terrain with sinusoidal height of the body with body's orientation.

- General case: We take credit from the redundancy of the HWR's body, namely we can activate all its degrees of freedom for the sake of providing the HWR with any given orientation during the walking process, which results in avoiding the encountered obstacles, where this orientation is inevitably required as the oriented posture given in Figure 31.

5 Conclusion

The proposed walking algorithm for the HWR on irregular terrain, based on the key elements of modeling the robot and its legs, modeling the terrain, adapting the legs to

the terrain, synchronizing the legs for a tripod gait, and ensuring compatibility with the body's movement, shows promising results. The algorithm is demonstrated to be accurate and reliable in following the shape of irregular terrains, regardless of the terrain type or leg and body trajectories.

One of the major advantages of this algorithm is its applicability to various types of legged robots, including jumpers, bipeds, quadrupeds, and hexapods, due to the utilization of the HWR's redundancy and activation of all degrees of freedom of the robot's body.

Future perspectives for this research could include testing the algorithm on a real robot with data from real terrains to validate its performance in real-world conditions. Additionally, further investigation of the walking stability of the HWR in relation to terrain irregularities could provide valuable insights for enhancing the algorithm's performance.

Overall, this research contributes to the advancement of robot control for complex geometries and irregular terrains, paving the way for improved locomotion capabilities of legged robots in challenging environments.

References

[1] R. D. Quinn, G. M. Nelson, R. J. Bachmann, D. A. Kingsley and R. E. Ritzmann. Insect designs for improved robot mobility. *Proc. 4th Int. Conf. On Climbing and Walking Robots* (2001) 69–76.

[2] K. Lagaza. A Literature Review on Motion Planning of Hexapod Machines Using Different Review Article - Mechanical Engineering A Literature Review on Motion Planning of Hexapod Machines Using Different Soft Computing Methods. *Global Journal of Engineering, Science and Social Science Studies* **3** (1) (2018) 1–10.

[3] X. Ding, Z. Wang, A. Rovetta and J. M. Lagaza. Locomotion Analysis of Hexapod Robot. *Climbing and Walking Robots* (2010) 291–312. https://doi.org/10.5772/8822

[4] D. Wettergreen and B. D. Wettergreen. Robotic walking in natural terrain Gait planning and behavior-based control for statically-stable walking robots. *IEEE International Conference on Intelligent Robots and Systems, December* (1995) 134.

[5] S. S. Nair. Modeling and simulation of a six-legged walking robot power system. *Simulation* **58** (3) (1992) 185–195.

[6] I. Doroftei and Y. Baudoin. A concept of walking robot for humanitarian demining. *Industrial Robot: An International Journal* **39** (5) (2012) 441–449. https://doi.org/10.1108/01439911211249733.

[7] G. Heppner, A. Roennau, J. Oberländer, S. Klemm and R. Dillmann. Laurope-six legged walking robot for planetary exploration participating in the spacebot cup. *WS on Advanced Space Technologies for Robotics and Automation* **2** (13) (2015) 69–76.

[8] F. Tedeschi and G. Carbone. Design Issues for Hexapod Walking Robots. *Robotics* **2014** (3) (2014) 181–206. https://doi.org/10.3390/robotics3020181.

[9] M. Billah, M. Ahmed and S. Farhana. Walking Hexapod Robot in Disaster Recovery : Developing Algorithm for Terrain Negotiation and Navigation. *International Journal of Mechanical and Mechatronics Engineering* **2** (6) (2008) 795–800.

[10] F. Zhang, S. Zhang, Q. Wang, Y. Yang and B. Jin. Straight Gait Research of a Small Electric Hexapod Robot. *Applied science* **11** (8) (2021) 3714.

[11] R. Ramirez, A. Arellano-Delgado, R. M. Lopez-Gutierrez, J. Pliego-Jimenez and C. Cruz-Hernández. Master-Slave Synchronization of a Planar 2-DOF Model of Robotic Leg. *Nonlinear Dynamics and Systems* Theory **21** (4) (2021) 420–433.

[12] J. Coelho, F. Ribeiro, B. Dias, G. Lopes and P. Flores. Trends in the control of hexapod robots: A survey. *Robotics* **10** (3) (2021) 1–22. https://doi.org/10.3390/robotics10030100.

[13] H. Cruse, T. Kindermann, M. D. Schummand and J. Schmitz. Walknet – a biologically inspired network to control six-legged walking. *Neural networks.* **11** (7-8) (1998) 1435–1447.

[14] W. Qidi, L. I. U. Chengju, Z. Jiaqi and C. Qijun. Survey of locomotion control of legged robots inspired by biological concept. *Information Sciences* **52** (10) (2009) 1715–1729.

[15] G. Figliolini and P. Rea. *Mechanics and Simulation of Six-Legged Walking Robots.* INTECH Open Access Publisher, 2007.

[16] K. Priandana and A. Buono. Hexapod Leg Coordination using Simple Geometrical Tripod-Gait and Inverse Kinematics Approach. *In International Conference on Advanced Computer Science and Information Systems (ICACSIS)* (2017) 35–40.

[17] R. Wang. Hybrid Gait Planning of a Hexapod Robot. *Modern Electronic Technology* **4** (2) (2020), 11. https://doi.org/10.26549/met.v4i2.5075.

[18] H. Xia, X. Zhang and H. Zhang. A new foot trajectory planning method for legged robots and its application in hexapod robots. *Applied Sciences (Switzerland)* **11** (19) (2021). https://doi.org/10.3390/app11199217.

[19] S. I. Beaber, A. S. Zaghloul, M. A. Kamel and W. M. Hussein. Dynamic modeling and control of the hexapod robot using matlab simmechanics. *ASME International Mechanical Engineering Congress and Exposition* (2018) 52033.

[20] B. Stanczyk and J. Awrejcewicz. Six-Legged Robot Gait Analysis. *Nonlinear Dynamics and Systems Theory* **15** (1) (2015) 63–72.

[21] C. Mahfoudi, K. Djouani, S. Rechak and M. Bouaziz. Optimal force distribution for the legs of an hexapod robot. *Proceedings of 2003 IEEE Conference on Control Applications, 2003. CCA* 1 (2003) 657–663.

[22] H. M. Schepers, E. H. F. Van Asseldonk, J. H. Buurke and P. H. Veltink. Ambulatory estimation of center of mass displacement during walking. *IEEE Transactions on Biomedical Engineering* **56** (4) (2009) 1189–1195.

[23] T. Wöhrl, L Reinhardt and R. Blickhan. Propulsion in hexapod locomotion: how do desert ants traverse slopes. *Journal of Experimental Biology* **220** (9) (2017) 1618–1625.